The H Lyman-? actinic flux in the middle atmosphere

Th. Reddmann, R. Uhl

Atmos. Chem. Phys. Discuss., 2, 1635–1654, 2002
www.atmos-chem-phys.org/acpd/2/1635/

Atmospheric Chemistry and Physics Discussions

The H Lyman-α actinic flux in the middle atmosphere

Th. Reddmann and R. Uhl

Institute of Meteorology and Climate Research, Forschungszentrum Karlsruhe und Universität Karlsruhe, Germany

Received: 12 September 2002 – Accepted: 11 October 2002 – Published: 28 October 2002

Correspondence to: Th. Reddmann (thomas.reddmann@imk.fzk.de)

Abstract

The penetration of solar H Lyman-α radiation into the terrestrial middle atmosphere is studied in detail. The Lyman-α actinic flux is calculated with a Monte Carlo approach including multiple resonance scattering of Lyman-α photons within the terrestrial atmosphere and a temperature dependent absorption cross section of molecular oxygen. The dependence of the actinic flux on the temperature profile is significant for O_2 column densities greater than about $10^{24}\,m^{-2}$. For column densities greater than about $5 \cdot 10^{24}\,m^{-2}$ resonance scattering becomes important at solar zenith angles $> 60^{\circ}$. The $O(^1D)$ quantum yield of the O_2 dissociation by Lyman-α photons is found to decrease from 0.58 in the lower thermosphere to 0.48 in the lower mesosphere. Parameterisations for Lyman-α actinic flux, mean O_2 absorption cross section and $O(^1D)$ quantum yield including temperature dependence and resonance scattering are given valid up to a O_2 column density of about $10^{25}\,m^{-2}$.

1. Introduction

The solar variability has a strong spectral dependence, with greater variation in the extreme UV part of the solar spectrum. Most of this radiation cannot penetrate the mesosphere and the uppermost stratosphere through the strong absorption by molecular oxygen. By chance, the highly variable and UV dominant solar hydrogen Lyman-α line at 121.6 nm coincides with a deep minimum of the O_2 absorption cross section. This gives Lyman-α photons a dominating role for photolysing CH_4, CO_2, and H_2O in the mesosphere.

Within most models of the middle atmosphere the Lyman-α flux is parameterised by a simple exponential (e.g. Nicolet, 1984). Chabrillat and Kockarts (1997) showed that such parameterisations are not sufficient to describe the Lyman-α flux in the mesosphere, because the O_2 absorption cross section has a temperature dependence which in addition varies over the spectrally resolved solar Lyman-α line profile. They give an

ACPD
2, 1635–1654, 2002

improved parameterisation based on a sum of exponentials of the O_2 (slant) column. In fact, their scheme does not include a detailed treatment of solar zenith angle dependence and the dependence of seasonal changes of the temperature profile within the mesosphere. In addition, determination of the Lyman-α actinic flux (which is equivalent to the photon number density) is complicated by Lyman-α resonant scattering in the terrestrial atmosphere, which gives rise to a prominent diffuse Lyman-α field.

These effects are not included in parameterisations used in models of the middle atmosphere. Calculations of the Lyman-α dayglow in the thermosphere have peen performed by different authors (see e.g. Bishop, 1999; Bush and Chakrabarti, 1995; Meier, 1991), but those studies do not reach into the mesosphere and do not include the temperature dependence of the O_2 absorption. As in the mesosphere the optical depth for Lyman-α absorption is high, even small changes in the outer conditions may produce observable effects in the photolysis rates. The evaluation of the importance of these effects demands a detailed wavelength dependent description combining scattering and absorption processes of Lyman-α photons within the atmosphere. For that purpose, a Monte Carlo program (MCP) was developed which takes into account the temperature dependent absorption by molecular oxygen and multiple resonance scattering by atomic hydrogen within the terrestrial atmosphere.

2. Description of the method

In order to determine the path of a single photon, first its wavelength is determined randomly, according to the solar line profile. Then the altitude of absorption or scattering is calculated randomly, as well as whether absorption or scattering occurs, according to the absorption coefficients of O_2 and H. Resonant scattering is treated with frequency redistribution caused by the associated Doppler effect but the natural linewidth is neglected. In case of scattering the path of the photon is continued with a random new direction and a new wavelength. As we are mainly interested in the mesosphere, a plane parallel atmosphere is assumed. Bush and Chakrabarti (1995) compare plane

ACPD
2, 1635–1654, 2002

parallel and spherical calculations and show that up to about 70° solar zenith angle the difference between two method is less than 10%, which is sufficient in the context of our study. For higher solar zenith distances the plane parallel version underestimates the contribution of scattered photons. To include resonantly scattered photons in the exosphere the outer boundary for the model is set at 1000 km. For each parallel layer the temperature and the densities of O_2 and H are taken from the MSIS-90 model of Hedin (1991).

In our calculations we consider 10^9 photons for each run. To determine the actinic flux and the photodissociation rates of O_2 we add the contributions of every photon along its path, using an altitude grid of 1 km resolution and a wavelength grid of 0.0004 nm resolution.

Whereas for the determination of the dissociation rates of H_2O, CH_4 and other species the integrated actinic flux is sufficient, the O_2 dissociation rate is determined within the model as the integration over the Lyman-α spectrum. In addition, Lacoursière et al. (1999) showed that the $O(^1D)$ yield of Lyman-α absorption is wavelength dependent, too. The determination of this yield is also included in the MCP module.

2.1. Solar H Lyman-α emission profile

First the initial wavelength λ of the photon is determined randomly. We assume that the solar H Lyman-α spectral distribution is proportional to

$$\exp\left(-\frac{(\lambda-\lambda_0)^2}{2s_1^2}\right)\cdot\left(1-a\exp\left(-\frac{(\lambda-\lambda_0)^2}{2s_2^2}\right)\right)$$

(self-reversed gaussian profile) with $\lambda_0 = 121.567$ nm, $s_1 = 0.0248$ nm, $s_2 = 0.0172$ nm, $a = 0.7153$, according to Scherer et al. (2000) (standard case, see their Fig. 2). Thus λ may be determined by the Neumann's rejection method: Calculate randomly

$$\lambda = \lambda_0 + s_1 \cos(2\pi\,\mathrm{ran})\sqrt{-2\ln\,\mathrm{ran}}$$

ACPD
2, 1635–1654, 2002

(Box-Muller method) again and again until

$$\text{ran} > a \exp\left(-\frac{(\lambda-\lambda_0)^2}{2s_2^2}\right)$$

is satisfied. All ran's denote (different) independent real random variables with a uniform distribution on $[0, 1]$.

Now the photon with the just calculated wavelength λ enters the top of the atmosphere. The angle of incidence is the solar zenith angle χ.

2.2. Extinction of the photon

We assume that the photon now starts in general in some altitude z with some wavelength λ and with some angle ϕ (between 0 and 180°) to the downward directed vertical line.

Then the coefficients for scattering, absorption, extinction, i.e. α_H, α_{O_2}, $\alpha_0 = \alpha_H + \alpha_{O_2}$, are calculated for the current wavelength λ at the grid altitude z_0 within the layer in which the photon just moves. For atomic hydrogen we use the scattering cross section

$$\sigma_H = \frac{f_{12}\,\mu_0\,e^2\,\lambda_0^2}{4\sqrt{\pi}\,m_e\,\Delta\lambda_D}\,\exp\left(-\left(\frac{\lambda-\lambda_0}{\Delta\lambda_D}\right)^2\right)$$

(in SI units) with the absorption oscillator strength $f_{12} = 0.4163$ and the Doppler width $\Delta\lambda_D = \lambda_0\, v_{th}/c$ where $v_{th} = \sqrt{2kT/m_H}$ denotes the thermal velocity. The absorption cross section σ_{O_2} of molecular oxygen is taken from Lewis et al. (1983) by interpolation.

For simplicity the extinction coefficient α is assumed to vary exponential with respect to the altitude z' in the current layer, i.e. $\alpha = \alpha_0\, e^{-\gamma(z'-z_0)}$ where γ is assessed by the extinction coefficients of the two surrounding layers. Then the probability p', that the photon will reach any given altitude z' within the layer on the ray, satisfies $dp'/dz' =$

ACPD
2, 1635–1654, 2002

$\alpha p'/\cos\phi$. Since $p' = 1$ for $z' = z$, we conclude

$$\ln p' = -\frac{\alpha_0}{\gamma\cos\phi}\left(e^{-\gamma(z'-z_0)} - e^{-\gamma(z-z_0)}\right).$$

Thus the photon is absorbed or scattered in an altitude z_{new} which may be calculated for the moment by

$$z_{new} = z_0 - \frac{1}{\gamma}\ln\left(e^{-\gamma(z-z_0)} - \frac{\gamma\cos\phi}{\alpha_0}\ln \text{ ran}\right)$$

if the argument of the outer logarithm is positive, otherwise $z_{new} = \pm\infty$. But if z_{new} would lie outside of the current layer, then the altitude of escape is taken as the next starting altitude z, and all the computations above are made with the next layer, unless the photon escapes from the atmosphere.

When the photon is actually absorbed or scattered, all the photon densities in the layers between z and z_{new} are increased by an amount proportional to the length of the particular section on the ray.

Finally, the condition ran $< \alpha_{O_2}/\alpha_0$ decides whether the photon is now absorbed by some O_2 molecule. In that case the O_2 molecule is photodissociated, and the photodissociation rate of O_2 (in the actual layer) is increased, as well as the $O(^1D)$ yield according to the $O(^1D)/O$ fraction

$$1.08 - \frac{0.168}{0.11\sqrt{2\pi}}\exp\left(-\frac{(\lambda/\text{nm} - 121.623)^2}{2\cdot 0.11^2}\right),$$

which is given in Lacoursière et al. (1999) (for 121.46 to 121.67 nm).

2.3. Resonance scattering by H

We suppose now that the photon is not absorbed by O_2 but scattered by excitation of some H-atom.

First, the velocity $\boldsymbol{v}$ of the scattering H-atom has the component $v_1 = -c\,(\lambda - \lambda_0)/\lambda_0$ in the previous direction of the photon. The two other components (the last is assumed to be horizontal) are calculated randomly by $v_2 = r\cos\psi$ and $v_3 = r\sin\psi$ with $r = v_{\text{th}}\sqrt{-\ln \text{ran}}$ and $\psi = 2\pi\,\text{ran}$, according to the Maxwellian velocity distribution and the Box-Muller method.

For the angular dependence of the intensity of resonantly scattered radiation we refer to Chandrasekhar (1960). In case of the Lyman-α doublet one obtains $\frac{11}{12} + \frac{3}{12}\cos^2\theta$. Therefore the component n_1 (in the previous direction) of the photon's new (normalised) direction $\boldsymbol{n}$ has a probability density proportional to $11 + 3n_1^2$ on $[-1, 1]$. Thus n_1 may be determined by the Neumann's rejection method: Calculate randomly $n_1 = 2\,\text{ran} - 1$ again and again until $\text{ran} < (11 + 3n_1^2)/14$ is satisfied. Then calculate $n_2 = \cos\beta\sqrt{1 - n_1^2}$ and $n_3 = \sin\beta\sqrt{1 - n_1^2}$ where $\beta = 2\pi\,\text{ran}$.

This new direction $\boldsymbol{n}$ determines the photon's new angle ϕ_{new} to the vertical direction $\boldsymbol{n}_{\text{ver}}$ by $\cos\phi_{\text{new}} = \boldsymbol{n}\cdot\boldsymbol{n}_{\text{ver}} = n_1\cos\phi + n_2\sin\phi$, and the photon's new wavelength λ_{new} by $(\lambda_{\text{new}} - \lambda_0)/\lambda_0 = -\boldsymbol{n}\cdot\boldsymbol{v}/c$, which implies $\lambda_{\text{new}} = \lambda_0 - \lambda_0(n_1v_1 + n_2v_2 + n_3v_3)/c$.

Finally, the photon may be now considered to start once more, but with z_{new}, λ_{new}, ϕ_{new} replacing z, λ, ϕ. This loop terminates when the photon is absorbed by O_2 or escapes from the atmosphere. Then the next photon is considered.

3. Results

For different climatological situations the spectral distribution of the normalised actinic flux

$$\hat{Q} = \frac{Q}{Q_\infty}$$

has been calculated, where Q denotes the actinic flux of the Lyman-α line, and Q_∞ the corresponding solar flux outside the atmosphere. The T-, O_2- and H-profiles for

equinoctial and solstitial conditions have been taken from the MSIS model (Hedin, 1991) and refer to solar minimum conditions.

3.1. Spectral evolution

Figure 1 shows two examples of the spectral evolution of the normalised actinic flux. One outstanding feature is the resonance peak seen at an altitude of 200 km at the line centre for solar zenith angle $\theta = 0^{\circ}$. It demonstrates the effect of resonance scattering in the terrestrial atmosphere. Lower in the atmosphere, the scattered photons having a longer path in the atmosphere are absorbed by O_2 with a higher probability. This causes the sharp absorption feature near the line center seen at 90 km altitude and below. The spectral dependence of O_2 absorption causes the asymmetry of the line shape there.

For high solar zenith angles, the spectrum already at 200 km starts with an absorption feature. This is caused in the high atmosphere by scattering photons to space. Due to the higher temperature there, this occurs in a wider spectral range. The double peaked spectrum at very low altitudes is caused by Lyman-α photons resonantly scattered in the high atmosphere downwards, therefore experiencing a smaller O_2 column density compared to the direct solar beam.

3.2. Actinic flux

The normalised actinic flux $\widehat{Q}$ has been calculated by integration of the spectral distribution and is shown in Fig. 2 as a function of O_2 column density for combinations of date, latitude and solar zenith angle as noted. Here and the following, always the slant column is given. For O_2 columns higher than $10^{25}\,\mathrm{m}^{-2}$ the effects of scattering are clearly dominant for high solar zenith angles.

Nicolet (1985) and Chabrillat and Kockarts (1997) give approximations of the Lyman-α actinic flux within the mesosphere. The temperature dependence of the O_2 absorption coefficient is accounted for by a corrected column density or by a sum of exponen-

ACPD
2, 1635–1654, 2002

tials, respectively, but only for a fixed temperature profile.

To account for different temperature profiles and in order to include the contribution of scattered photons we use the parameterisation

$$\widehat{Q} = f\,\mathrm{e}^{-\overline{\tau}} + \widehat{Q}_\mathrm{s} \tag{1}$$

with the mean optical depth

$$\begin{aligned}\overline{\tau} = {} & (2.48\cdot 10^{-22} + 6\cdot 10^{-26}\,\mathrm{K}^{-1}\,T_1)\,(\mathrm{m}^2\,N)^{0.9} \\ & -(2.6\cdot 10^{-25} - 10^{-27}\,\mathrm{K}^{-1}\,T_2)\,\mathrm{m}^2\,N \\ & +2.5\cdot 10^{-51}\,\mathrm{m}^4\,N^2\end{aligned}$$

depending on the O_2 (slant) column density N, essentially. T_1 and T_2 denote the temperature where the O_2 column density is $N_1 = 10^{24}\,\mathrm{m}^{-2}$ or $N_2 = 6\cdot 10^{24}\,\mathrm{m}^{-2}$, respectively. The factor

$$f = 1 + 0.07\,(\cos\chi - 0.5)\exp(-4\cdot 10^{-24}\,\mathrm{m}^2\,N)$$

gives the variations with respect to the solar zenith angle χ at low O_2 column densities. The addend

$$\widehat{Q}_\mathrm{s} = 0.005\,(\cos\chi + 0.07)\cdot\exp\left(-\,9.8\cdot 10^{-25}\,\mathrm{m}^2\,N\,(\cos\chi + 0.02)\right)$$

gives the contribution of scattering for higher solar zenith angles at high O_2 column densities.

Figure 3 shows the comparison of the MCP results with the parameterisation for the set of combinations of date, latitude and solar zenith angle as given, together with the specific temperature profiles. Up to a column density of O_2 of about $10^{25}\,\mathrm{m}^{-2}$ the deviations between exact and approximate solution are less than 5%. In addition, the parameterisation of Chabrillat and Kockarts (1997) is shown in Fig. 3 for comparison. For small O_2 columns the effect of resonance scattering is less than about 5%, whereas the influence of different temperature profiles exceeds 5% above $2\cdot 10^{24}\,\mathrm{m}^{-2}$

ACPD
2, 1635–1654, 2002

for cases where the temperature deviates from standard conditions. Further tests show that the parameterisation gives results within 20% compared with the MCP results for attenuations > 10^{-6} for the cases studied.

3.3. O_2 photodissociation

Figure 4 shows the normalised O_2 photodissociation

$$\widehat{J}_{O_2} = \frac{J_{O_2}}{Q_\infty}$$

as a function of altitude for different cases, calculated by the Monte Carlo program. The mean O_2 absorption cross section defined by

$$\overline{\sigma}_{O_2} = \frac{J_{O_2}}{n_{O_2} Q} = \frac{\widehat{J}_{O_2}}{n_{O_2} \widehat{Q}}$$

is shown in Fig. 5. It can be approximated by the parameterisation

$$\begin{aligned}\overline{\sigma}_{O_2} = {} & 0.765 \cdot 10^{-24}\,\mathrm{m}^2 \cdot \left(1 + 0.35 \exp(-5 \cdot 10^{-25}\,\mathrm{m}^2\, N)\right) \\ & \cdot \left(1.1 + 0.1 \tanh(3 \cdot 10^{-25}\,\mathrm{m}^2\, N\, (0.8 - \cos\chi)^+ - 2.4)\right) \\ & \cdot \left(1.16 - 0.0021\,\mathrm{K}^{-1}\, T + 6 \cdot 10^{-6}\,\mathrm{K}^{-2}\, T^2\right) \qquad (2)\end{aligned}$$

with the function $x^+ = \max(x, 0)$. For comparison in Fig. 6 the ratio of this parameterisation to the mean O_2 absorption cross section $\overline{\sigma}_{O_2}$ derived from the MCP results is shown.

3.4. Yield of $O(^1D)$

The dissociation of O_2 has the form

$$O_2 + h\nu \begin{array}{l} \nearrow O(^3P) + O(^3P) \\ \searrow O(^3P) + O(^1D) \end{array}$$

ACPD
2, 1635–1654, 2002

Lacoursière et al. (1999) showed that the O(^1D) quantum yield of Lyman-α photons absorption strongly varies over the absorption feature near the Lyman line. It decreases from 1 shortward of the absorption feature, to less than 0.5 at the feature center and rises again to 0.7 at longer wavelengths. As the spectral form of the Lyman-α line changes with height within the atmosphere (see Sect. 3.1) the O(^1D) yield is also height dependent. The corresponding mean O(^1D) quantum yield $\bar{\Phi}_{O(^1D)}$ defined as the fraction O(^1D)/O of the yields of the whole line is given in Fig. 7 for different atmospheric situations. It is 0.58 in the lower thermosphere and decreases to 0.48 in the lower mesosphere. For high solar zenith angles it increases again to 0.54, which is caused by resonantly scattered photons near the Lyman-α line center.

$\bar{\Phi}_{O(^1D)}$ can be parameterised in that region by the expression

$$\bar{\Phi}_{O(^1D)} = 0.48\left(1 + 0.2\exp(-3\cdot 10^{-25}\,\mathrm{m}^2\,N)\right) \cdot\left(1.06 + 0.06\tanh(3.5\cdot 10^{-25}\mathrm{m}^2\,N\,(0.8 - \cos\chi)^+ - 2.4)\right)$$

4. Conclusions

Two effects influencing the actinic flux at the H Lyman-α line in the middle atmosphere have been studied in our analysis: First, the variation of the temperature profile causes significant changes of the solar H Lyman-α actinic flux for O_2 columns greater than about $10^{24}\,\mathrm{m}^{-2}$. Parameterisations of the actinic flux for such high O_2 columns should include corrections for the actual temperature profile. We remark that even for a fixed profile there is a change of the temperature as a function of column by the varying solar zenith angle. As the column is the parameter in most parameterisations, also in that case the temperature profile changes. The second effect on the actinic flux studied is resonance scattering. It can be separated in two spatial regimes: for low O_2 column densities ($< 10^{23}\,\mathrm{m}^{-2}$) the actinic flux decreases by about 7% from low to high solar zenith angles. For high column densities ($> 5\cdot 10^{24}\,\mathrm{m}^{-2}$) and solar zenith

ACPD
2, 1635–1654, 2002

angles > 60° the actinic flux is increased by resonance scattering compared to the case without scattering. For very high solar zenith angles actinic flux is even dominated by scattered photons at column densities > 10^{25} m^{-2}. Our new parameterisation includes both effects and agrees with the MCP result within 5% up to 10^{25} m^{-2}, but using plane parallel geometry the actinic flux for very high solar zenith angles is possibly underestimated. Chabrillat and Kockarts (1997) claim for their parameterisation an accuracy better than 2% up to 10^{25} m^{-2}. This statement neglects the influence of different temperature profiles and resonance scattering.

There are additional factors influencing the actinic flux. The shape of the solar Lyman-α line shape is known to change with the solar cycle (Vidal-Madjar, 1975). Especially the primary central depression may depend on solar activity, as does a slight asymmetry of the line. Both effects can be included in our program, but as reliable data are missing, this influence has been neglected in our study. In addition, the temperature and hydrogen density in the thermosphere and exosphere depend on solar activity, and so does the exact contribution of scattered radiation.

From a chemical point of view, resonantly scattered photons may have effects especially for the concentration of CH_4 which is dominantly destroyed by Lyman-α photons. In addition, during daylight conditions the $O(^1D)$ concentration may be affected in the mesosphere. Here also the varying $O(^1D)$ yield must be considered for photochemical calculations. By implementation of our parameterisation in chemical models of the upper stratosphere and mesosphere this can be tested.

Acknowledgements. This work is a contribution to the project KODYACS of the AFO2000 framework and funded by the Bundesministerium für Bildung und Forschung.

References

Bishop, J.: Transport of resonant atomic hydrogen emissions in the thermosphere and geocorona: model description and applications, J. Quant. Spect. Rad. Transfer, 61, 473–491, 1999. 1637

Bush, B. C. and Chakrabarti, S.: A radiative transfer model using spherical geometry and partial frequency redistribution, J. Geophys. Res., 100, 19 627–19 642, 1995. 1637
Chabrillat, S. and Kockarts, G.: Simple parameterization of the absorption of the solar Lyman-α line, Geophys. Res. Lett., 24, 2659–2662, 1997. 1636, 1642, 1643, 1646, 1650
Chandrasekhar, S.: Radiative Transfer, Dover, 1960. 1641
Hedin, A. E.: Extension of the MSIS thermosphere model into the middle and lower atmosphere, J. Geophys. Res., 96, 1159–1172, 1991. 1638, 1642
Lacoursière, J., Meyer, S. A., Faris, G. W., Slanger, T. G., Lewis, B. R., and Gibson, S. T.: The O(^1D) yield from O_2 photodissociation near H Lyman-α (121.6 nm), J. Chem. Phys., 110, 1949–1958, 1999. 1638, 1640, 1645
Lewis, B. R., Vardavas, I. M., and Carver, J. H.: The aeronomic dissociation of water vapor by solar H Lyman α radiation, J. Geophys. Res., 88, 4935–4940, 1983. 1639
Meier, R. R., Ultraviolet spectroscopy and remote sensing of the upper atmosphere, Space Sci. Rev., 58, 1–185, 1991. 1637
Nicolet, M.: Photodissociation of molecular oxygen in the terrestrial atmosphere: Simplified numerical relations for the spectral range of the Schumann-Runge bands, J. Geophys. Res., 89, 2573–2582, 1984. 1636
Nicolet, M.: Aeronomical aspects of mesospheric photodissociation: Processes resulting from the solar H Lyman-alpha line, Planet. Space Sci., 33, 69–80, 1985. 1642
Scherer, H., Fahr, H. J., Bzowski, M., and Ruciński, D.: The influence of fluctuations of the solar emission line profile on the Doppler shift of interplanetary $H_{Ly\alpha}$ lines observed by the Hubble-Space-Telescope, Astrophys. Space Sci., 274, 133–141, 2000. 1638
Vidal-Madjar, A.: Evolution of the solar Lyman alpha flux during four consecutive years, Solar Phys., 40, 69–86, 1975. 1646

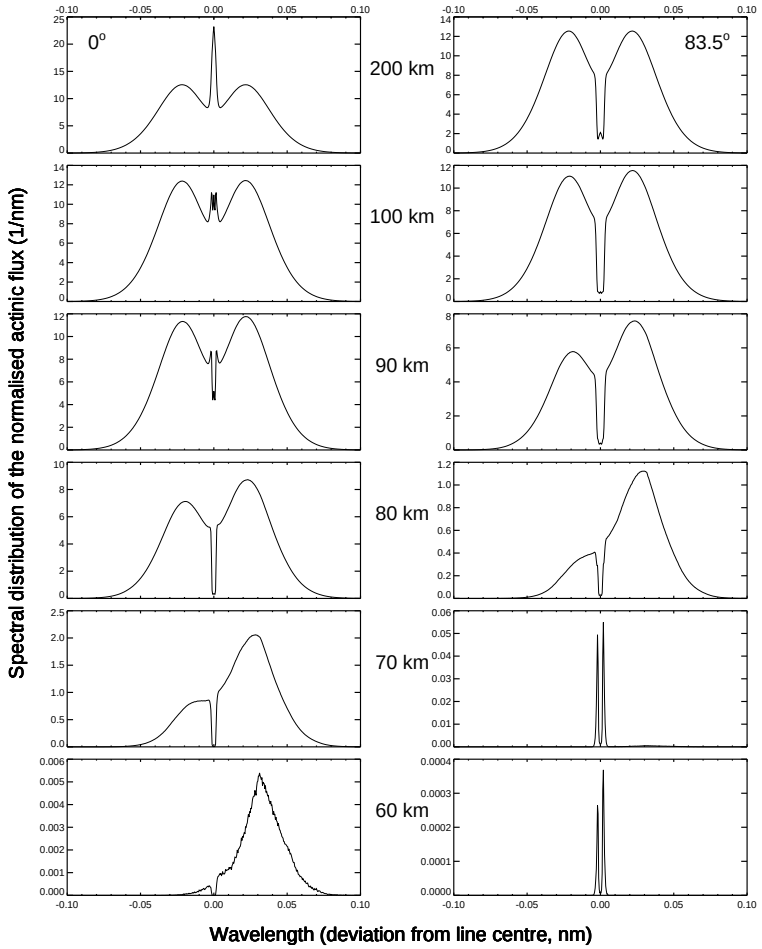

Fig. 1. Spectral evolution of the Lyman-α line for different altitudes at solar zenith angles $\chi = 0^{\circ}$ (left) and $\chi = 83.5^{\circ}$ (right). Integral over the solar line is set to 1. Note the different scales.

ACPD
2, 1635–1654, 2002

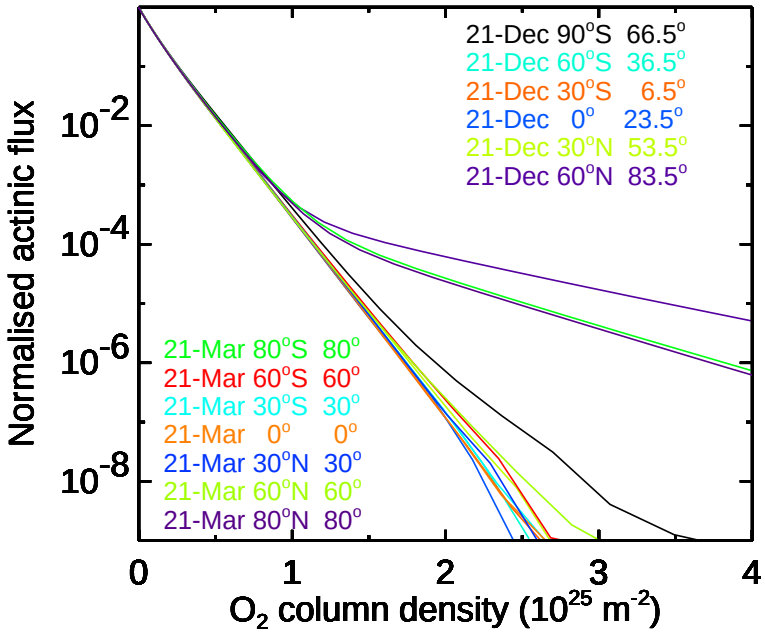

Fig. 2. Normalised actinic flux $\widehat{Q}$ of the Lyman-α line as a function of O_2 (slant) column for different combinations of date, latitude and solar zenith angle, calculated by the MCP.

ACPD
2, 1635–1654, 2002

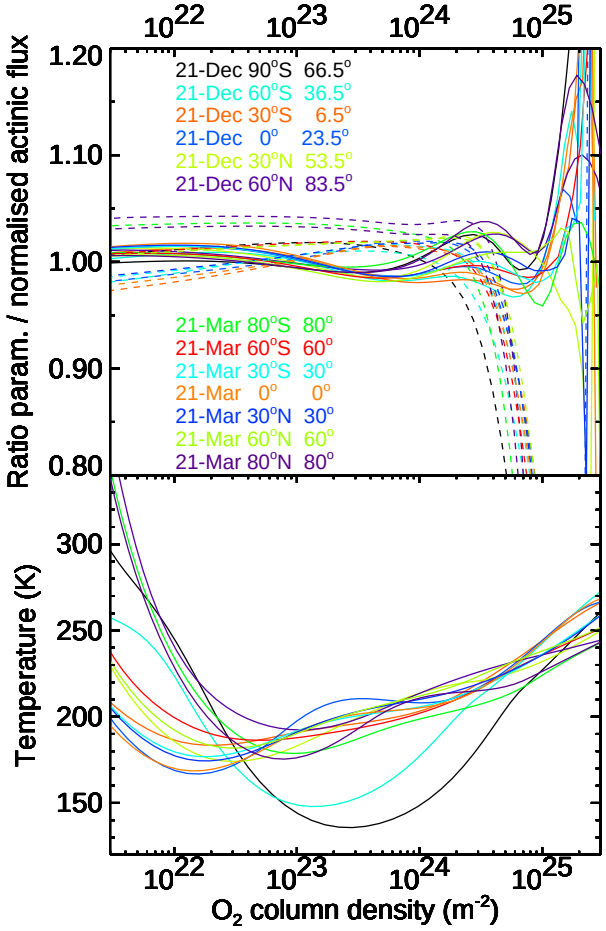

Fig. 3. Comparison of the MCP results for the normalised actinic flux $\widehat{Q}$ with the parameterisation Eq. (1). Dotted lines refer to the parameterisation of Chabrillat and Kockarts (1997). Below the corresponding temperature profiles are shown.

ACPD
2, 1635–1654, 2002

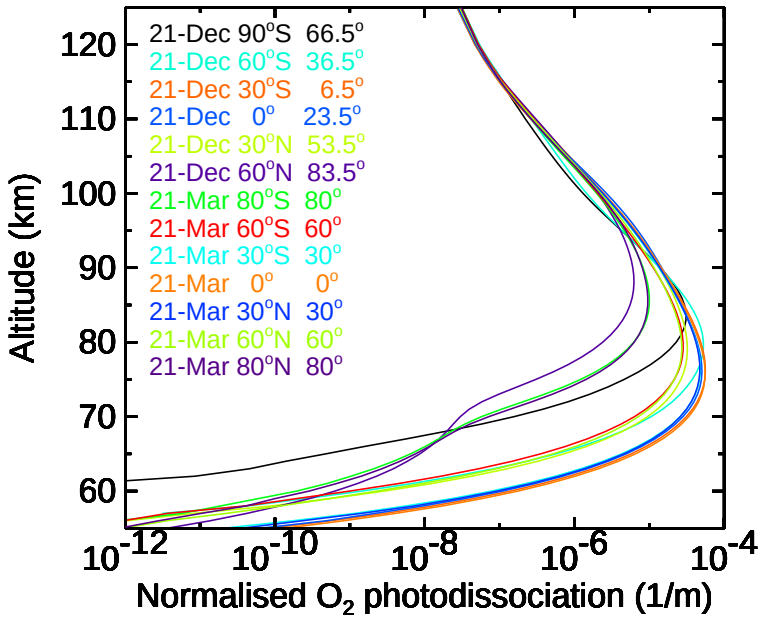

Fig. 4. Normalised O_2 photodissociation rate $\widehat{J}_{O_2}$ as a function of geometric altitude for different combinations of date, latitude and solar zenith angle, calculated by the MCP.

ACPD
2, 1635–1654, 2002

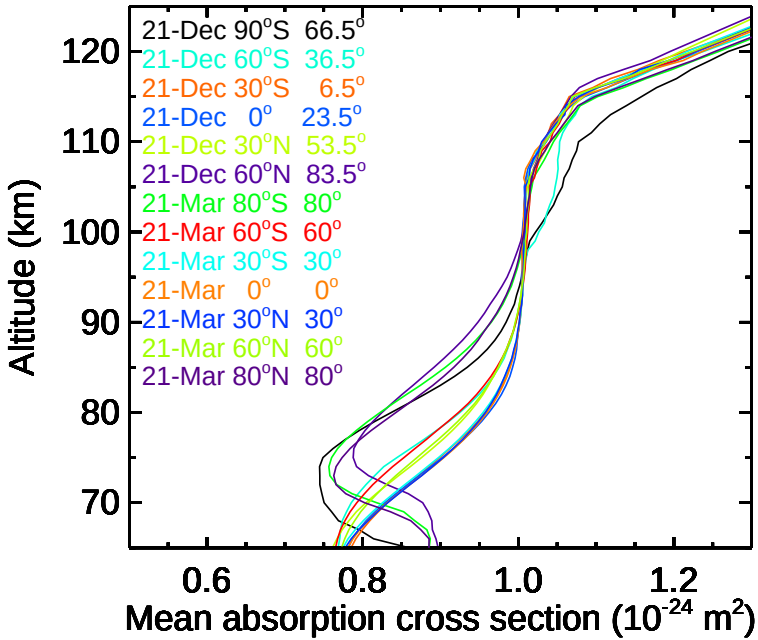

Fig. 5. Mean absorption cross section $\overline{\sigma}_{O_2}$ as a function of altitude.

ACPD
2, 1635–1654, 2002

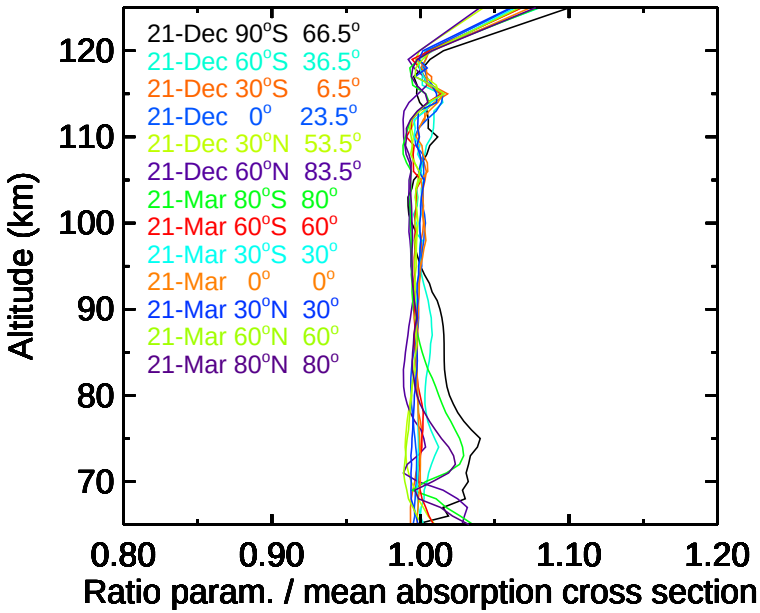

Fig. 6. Comparison of the MCP results for the mean absorption cross section $\overline{\sigma}_{O_2}$ with the parameterisation Eq. (2).

ACPD
2, 1635–1654, 2002

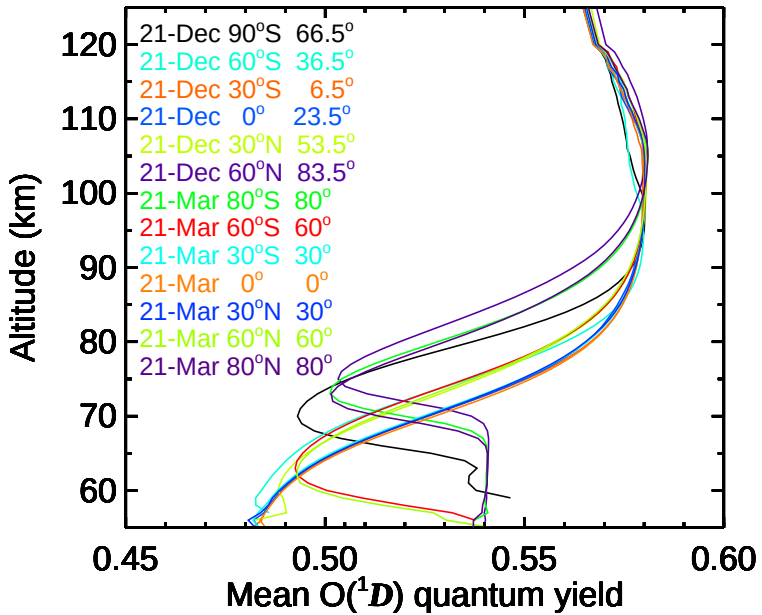

Fig. 7. Mean O(^1D) quantum yield $\bar{\Phi}_{O(^1D)}$ as a function of altitude, calculated by the MCP.

ACPD
2, 1635–1654, 2002